



1
2
3
4

EXPERIMENTAL INVESTIGATION OF NONLINEAR AERODYNAMIC DAMPING
OF PARTIAL AIRPLANE ASSEMBLY

O.E. ABDELHAMID *

ABSTRACT

Low speed wind tunnel testing of partial assemblies of aircraft fuselage and its horizontal tail surfaces are performed using a special dynamic stability balance. Experiments were aimed for investigating the effects of airplane aerodynamic components on the nonlinear behaviour of pitch damping in a range of moderate angles of attack. The function of balance is based on the method of forced pitch oscillations of geometrically similar model in straight parallel air flow. Damping coefficients are determined from analysis of motion records. Measurements are performed in range of flow velocities at different oscillation frequencies. Obtained results proved linear dependence of damping derivative on flow velocity, and independence of the nondimensional damping in pitch derivative on the oscillations nondimensional frequency. Strong nonlinearity in the dependence with angle of attack is observed, which is related to the creation and separation of vortices on fuselage sides. The research proved strong favourable contribution of quasi-slender fuselages to the nonlinear character of aerodynamic forces of their aircraft assemblies.

INTRODUCTION

Aerodynamic damping is a significant component of aircraft aerodynamic reactions. It plays a major role in damping its motion modes after disturbances and control applications. Its value is theoretically estimated in early stages of design and experimentally verified by testing in wind tunnels. For modern airplane designs, remarkable differences are noticed between theoretical and experimental results. These differences are referred to basic simplifying assumptions inherent in theory and to complexity characterizing the new design shapes. Main features of this complexity are the widened fuselages, enlarged pilot canopies, under or over body engine intakes, in addition to low aspect ratio wings and vortex strakes. These design renovations complicated the vortex pattern of flow around airplane body and led to rise of strong nonlinearities in their aerodynamic characteristics. Theoretical

* Department of Aeronautical Engineering, Military Technical College, Cairo, EGYPT



prediction of these nonlinearities is not yet well defined. These features of modern airplanes and their aerodynamic characteristics increased the dependence on experimental data for correct assessment of their flying qualities.

AERODYNAMIC DAMPING OF LONGITUDINAL OSCILLATIONS

During oscillations of airplane around a lateral axis passing through its center of gravity, pitching and angle of attack variations occur. Components of aerodynamic damping moment of this motion are the damping of pitch at constant incidence ω_y and the damping of vertical plunging $\dot{\alpha}$. Wing-body combination and horizontal tail surface contribute to both components. This relation is mathematically expressed in the form [1] :

$$(M_y^{\dot{\theta}})_{WB+HT} = (M_y^{\omega_y})_{WB} + (M_y^{\omega_y})_{HT} + (M_y^{\dot{\alpha}})_{WB} + (M_y^{\dot{\alpha}})_{HT} \quad (1)$$

where quantities between brackets are derivatives of pitching moment with respect to rates of pitching or plunging for either wing-body combination or horizontal tail surface. Damping of pitch at constant angle of incidence is due to aerodynamic effects that accompany airplane rotation. Its nondimensional derivative is given by [2] :

$$m_y^{\omega_y} = -\frac{2}{c^2} (x_{a.c.} - x_{c.g.}) | x_{a.c.} - x_{c.g.} | c_{y_{WB}}^{\alpha} - \frac{2L_T^2}{c^2} c_{y_{HT}}^{\alpha} \frac{S_{HT}}{S_W} \eta_{HT} \quad (2)$$

First term expresses the wing-body combination effect due to the change in angle of attack

$$\Delta \alpha = -\omega_y \left(\frac{x_{c.g.} - x_{a.c.}}{V} \right) \quad (3)$$

Second term is tail contribution. Damping of vertical plunging is caused by unsteady nature of resulting pressure distribution and lag of down-wash between wing and horizontal tail surface.

$$M_y^{\dot{\alpha}} = (M_{y_{WB}}^{\dot{\alpha}})_{U.E.} + (M_{y_{HT}}^{\dot{\alpha}})_{U.E.} + (M_{y_{HT}}^{\dot{\alpha}})_{D.L.} \quad (4)$$

Damping due to unsteady effects depends on frequency of oscillations, while the down-wash lag effect is dependent on relative position of tail with respect to wing. In cases of low frequency oscillations and wing absence, damping of oscillatory motion is only due to effects of pitching at constant incidence. This component is referred to as damping in pitch.

WIND TUNNEL TESTING POSSIBILITIES

Wind tunnels are the main experimental aerodynamics test facilities offering wide range of possibilities for measuring the damping derivatives. Geometrically similar models are oscillated in test section flow, with damping derivatives determined from analysis of motion or force measurements records. Both free and forced oscillation methods are used. Free oscillation methods, Fig. 1a, are characterized by its simplicity, but it has a main disadvantage that results represent a wide range of amplitude rather than a discrete value. When nonlinearities are of interest, amplitude of oscillations must be kept small, which affects the accuracy of results. Forced oscillation tests, Fig. 1b, are performed at constant amplitude, which can be arbitrarily chosen small. In the elastic forcing method, Fig. 1b, harmonic oscillations are imparted to the model through a linear spring. Damping is determined from forcing and forced motion amplitudes, frequency and phase shift. Excitation can be at amplitude or phase resonances with exciters of variable amplitude.

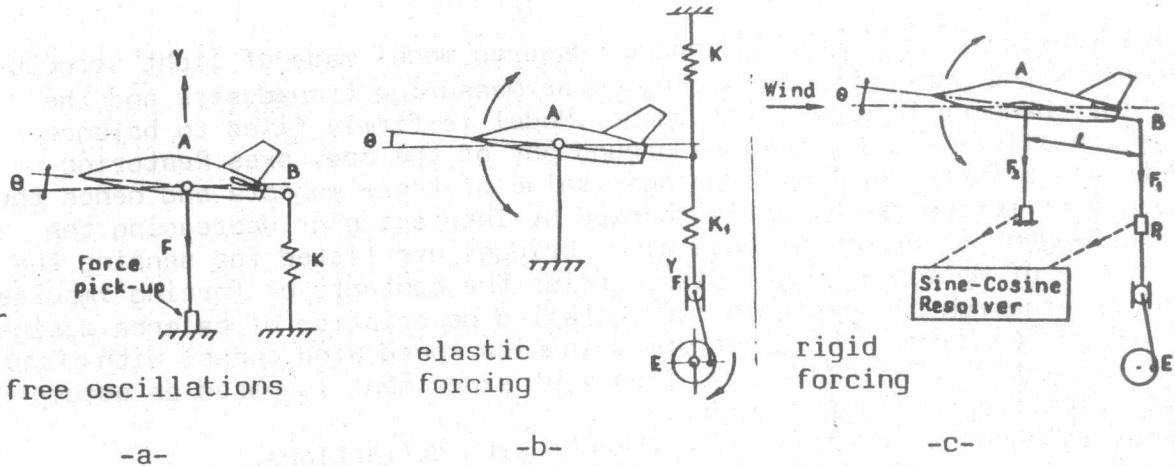


Fig.1 Different possibilities of measuring dynamic derivatives

system structural coefficients. Electrical excitation is preferred, as beside the possibility of amplitude control, it has favourable frequency stability and control characteristics. It enables self excitation at phase resonance and has the unique capability of dealing with negatively damped oscillations of dynamically unstable configurations.

In methods of rigidly forced oscillations, Fig. 1c, no spring elements are used in the system. Aerodynamic derivatives are determined from in and out of phase components of measured reactions. These reactions include large amplitude inertial forces and moments which are to be separated by repeating the tests in vacuum. Thus aerodynamic reactions are obtained as small differences between large vector quantities. Unless inertial reactions are well balanced, obtained results are of low accuracy. Equipments used for measuring dynamic derivatives in wind tunnel are known as dynamic stability balances. Complete review and analysis of dynamic stability derivatives measurements in wind tunnels are given in [3].

EXPERIMENTATION

A dynamic stability balance is used, function of which is based on method of elastic forcing with electrical excitation and damping evaluation from motion records.

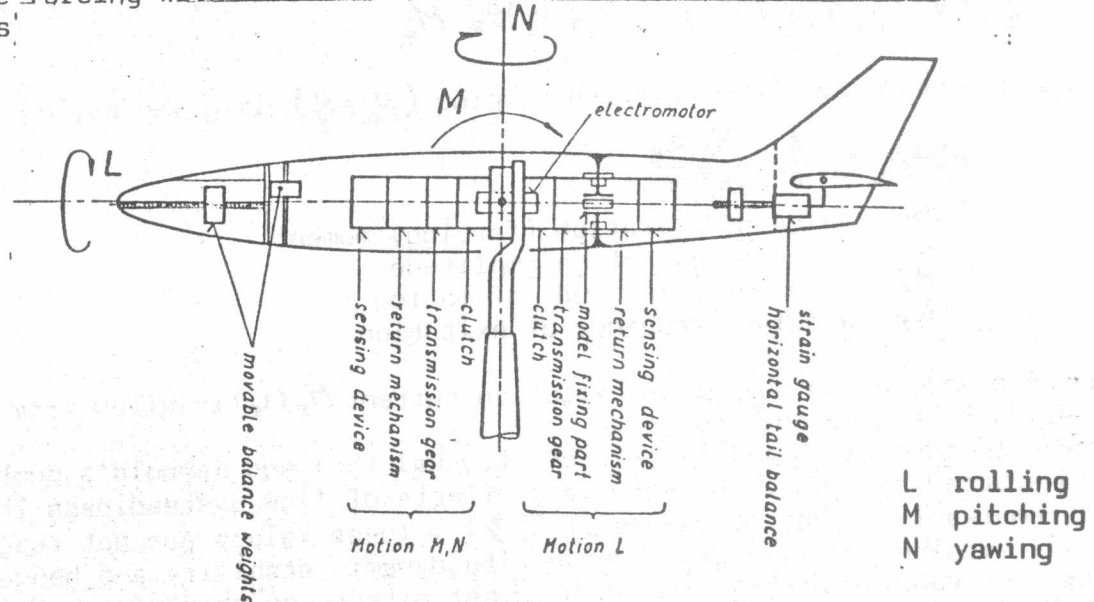


Fig.2 Scheme of model with stability balance installed.



Stability balance is installed inside measured model made of light structure. It contains the oscillations forcing motor, measuring transducers and the means for changing the motion frequency. Model is firmly fixed to balance body which allows angular motions around any of the body axes. Restoring moments are affected by sheet springs. Value of these moments and hence the frequency of motion are fluently changed by increasing or decreasing the working length of spring. Two Wheatstone bridges are fitted for sensing the time course of motion. A control disc carries the contacts of forcing impulse and of reverse run of forcing motors. Detailed description of balance design is given in [4]. Measuring is performed in a low speed wind tunnel with circular open test section of diameter 3m. Theory of experiment is based on assumptions:

- a-small amplitudes of oscillations.
- b-linear dependence of aerodynamic moments with deflections.
- c-linear variation of spring restoring moment with deflection.
- d-negligible model suspension effects and wind tunnel boundary corrections.
- e-friction damping is seperated by testing at zero tunnel speed.

Conditions at (a) are realized by the possibility of selecting duration of forcing contacts arbitrarily short. With this assumption valid, conditions at (b) are satisfied. Linear character of return springs is experimentally verified. Balance and body are supported by vertical strut of maximum diameter near body less than 30 mm, considered negligible with respect to body dimensions. Wind tunnel boundary corrections for slowly oscillating three-dimensional bodies in an open test section are negligibly small [5]. Friction damping of balance system is due to rolling friction in bearings, sliding friction in electric contacts, friction forces in toothed gearing, viscous friction in return spring guides and molecular friction of spring material. By repeating the no flow tests at different frequencies, it was found that damping moment dependence with friction is linear. Hence, friction damping seperation tests are to be performed at same frequency and angle of attack conditions of their corresponding tunnel on measurments. Fortunately, this linear dependence with frequency justified the combination of both friction and aerodynamic damping in a single term in the system's equation of motion.

According to previous assumptions, equation of motion of airplane model fixed to stability balance can be written in the form:

$$J_y \ddot{\theta} + (N_f + N_a) \dot{\theta} + (k_s + k_a) \theta = M_e \tag{5}$$

The sum of aerodynamic and friction damping $(N_a + N_f)$ is given by, [4]

$$N_f + N_a = \frac{4}{\pi} \frac{M_e a_e}{A_r^2 \omega_r} \tag{6}$$

- where
- M_e value of exitation (forcing) moment
 - a_e value of exitation amplitude
 - A_r resonance amplitude of motion
 - ω_r angular frequency of exitation

Dependence of exitation moment on exitation current $M_e(i_e)$ is given from motor characteristics and balance design.

Considered aerodynamic similarity is of Strauhal (St) and Reynold's numbers conditions. Strauhal number characterizes effects of flow unsteadiness. These effects remarkably appear at values of $St \geq 1$. These values are not reached during all airplane oscillatory modes of its dynamic stability and hence, not simulated in tunnel tests [6]. Reynold's number effects on aerodynamic damping in the linear range are small, but in range of aerodynamic nonlinearities, low



6

values of Reynold's number do not allow extrapolation of results to flight conditions.

RESULTS AND ANALYSIS

Measurements are performed on 1/4 scale model of an airplane fuselage with and without its horizontal tail surfaces. Models are tested in a range of angles of attack -4.0 to 8.1 degrees with elevator deflection angles adjusted to their corresponding values at equilibrium conditions. Flow velocity is varied in the range $V = 0.0$ to 25.0 m/s resulting in a range of nondimensional frequency $\omega_y \doteq 0.1$ to 0.3 . Damping derivatives are determined from equation (6) using motion and starting current records and the dependence of forcing moment on starting current, $M_e(i_e)$. Examples of resulting oscillographic record and the dependence $M_e(i_e)$ are given in Fig.3 Friction damping is separated using the zero flow velocity measurements.

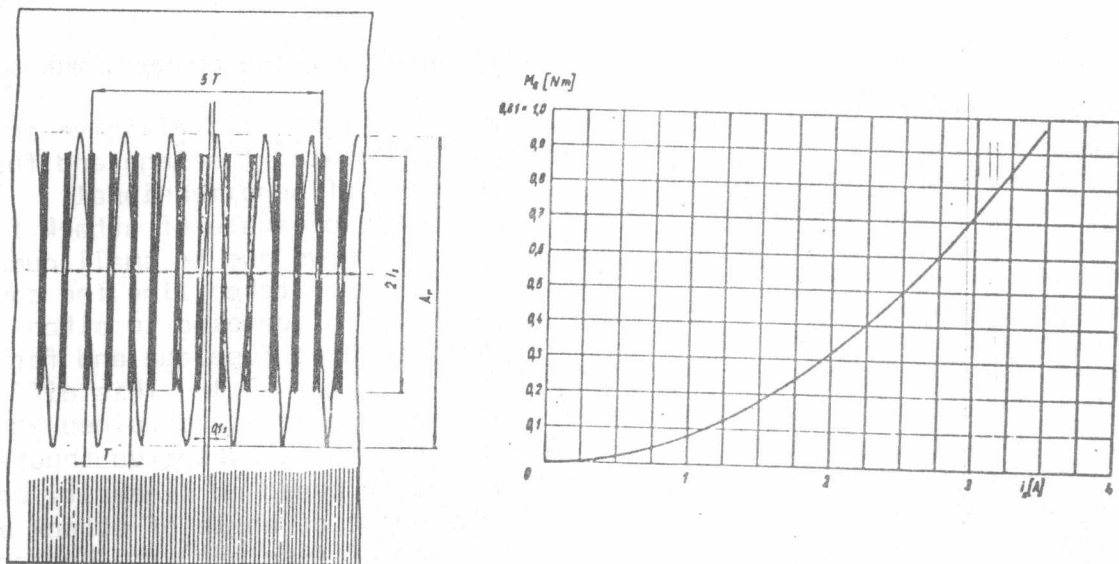


Fig.3 Example of resulting motion record and the dependence of excitation moment on excitation current

Dimensional aerodynamic damping in pitch derivative M_a is plotted as function of flow velocity V . To the measured values were fitted straight lines in all cases. Mean error of calculated slope was in the limits 2 to 8%. Large values are reached for the case of fuselage with horizontal tail surface. Example of results is shown in Fig.4.

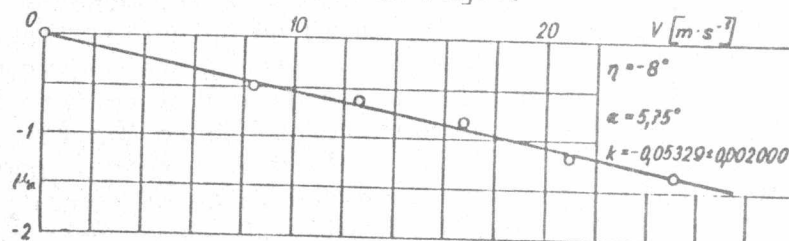


Fig.4 Dependence of dimensional damping derivative on flow velocity



By repeating the measuring of damping derivative at same value of velocity, mean square error of measurement was found to be in the range $< 3.8\%$. Nondimensional aerodynamic pitch damping derivative is given by

$$m_y^{\bar{\omega}_y} = \frac{\partial m_y}{\partial \bar{\omega}_y} = \frac{\partial m_y}{\partial (\omega_y \cdot L_T)} = \frac{2Ka}{8VFL_T^2} \quad (7)$$

Its value is plotted as function of nondimensional frequency $\bar{\omega}_y$ for the individual angles of attack. Example of results is shown in Fig.5. Fitted straight lines show independence of $m_y^{\bar{\omega}_y}$ on $\bar{\omega}_y$.

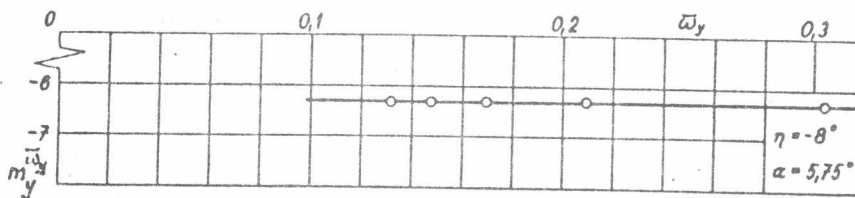


Fig.5 Dependence of nondimensional damping derivative on nondimensional frequency

In Fig.6a,b is shown the change of nondimensional damping derivative in dependence on angle of attack α for cases of isolated fuselage and fuselage with tail respectively. The results show that value of nondimensional derivative does not remain constant with the change of angle of attack for both cases. As the actual course of results is not known due to small number of measured points, measured values are connected by a broken line. The course of dependences $m_y^{\bar{\omega}_y}(\alpha)$ shows a change in the value of damping in pitch derivative $m_y^{\bar{\omega}_y} = +0.3$ to -1.5 for the isolated fuselage and for the fuselage with tail unit in the range $m_y^{\bar{\omega}_y} = -4.7$ to -7.1 . This difference has not a character of dispersion as each of these values is obtained as mean value of five measured points. In the same figure are also plotted theoretical results calculated according to slender body theory based on linearity consideration. By this theory, gained values are independent of angle of attack and higher than experimentally obtained ones for case of fuselage with horizontal tail. Two values for damping of isolated fuselage are obtained using slender body theory. First value assumes that fuselage rear part behind maximum area cross-section influences damping, while the second assumes its effect to be negligible due to boundary layer effects on potential flow pattern in this region.

It is clear that experimentally obtained results are substantially different from theoretical ones and prove the nonlinear character of variation of pitch damping with angle of incidence. For analysis of results in case of isolated fuselage we refer to eqn. (2). There is a change from positive values at $\alpha = 1.3^\circ$ to negative values for $0.2^\circ > \alpha > 1.8^\circ$. This is due to theoretically expected rearward position of fuselage aerodynamic center [7] slightly behind center of gravity. It is based on potential flow considerations at small incidences where viscous flow effects are negligible. Increasing angle of incidence in both positive and negative directions, the negative value of damping coefficient increases. With reference to eqn. (2), this increase is due to the nonlinear lift curve slope of fuselage gradually increasing with incidence [8]. Decreased absolute value of damping coefficient behind $\alpha = 3.4^\circ$ is referred to backward shift of aerodynamic center towards center of gravity. This shift accompanies the increasing tendency of created vortex pattern to sweep away boundary layer on fuselage rear part and restore

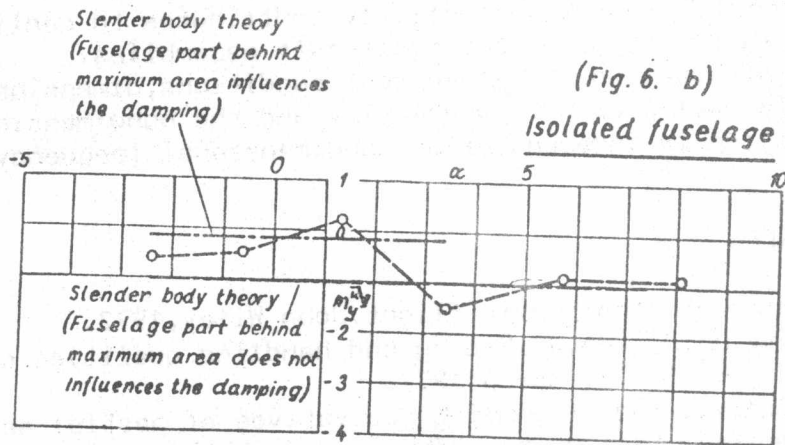
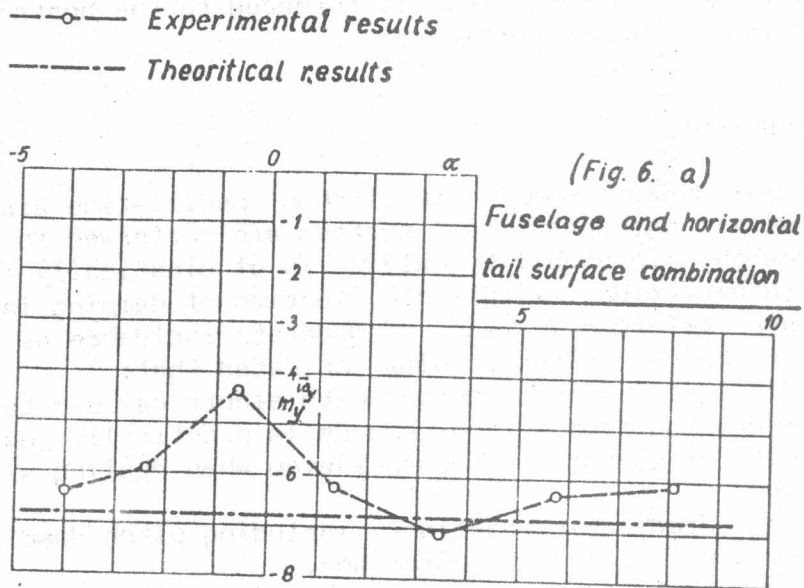


Fig.6 Nondimensional damping in pitch derivative as function of angle of attack for both tested configurations.

potential flow conditions. Results of measurements of fuselage with horizontal tail indicated increased pitch damping due to tail surface. This increase is in agreement with eqn. (2). Moreover, the line connecting results has similar course of variation to that of fuselage alone. This indicates that fuselage is the main contributor to fuselage tail combination nonlinearity. As the damping derivative is constant for linear air reactions, extent of its variation with incidence expresses the degree of air reactions nonlinearity. From fig. 6a, this variation reaches 2.85 compared to 1.75 in Fig. 6b for fuselage alone. With reference to eqn. (2), this higher value indicates induced nonlinearity in horizontal tail lift curve slope, caused by fuselage vortices, and representing additional interference effect to their combination. It is interesting to observe the horizontal tail surface effect on fuselage flow. It is manifested in the negative shift of incidence at minimum damping of the



near potential flow conditions. This is referred to the upstream induced tail upwash at rear fuselage portion.

CONCLUSIONS

Measurements of aerodynamic damping in pitch of oscillating airplane fuselage with and without its horizontal tail surface are performed in a low speed wind tunnel. Used dynamic stability balance is of elastically forced oscillations type with electrical excitation. Evaluation of damping is from motion records. Tests are performed in range of moderate incidence at low Reynold's and Strouhal's numbers. Obtained results indicated that:

- 1-Application of elastic forcing method with electrical excitation and evaluation of damping from motion records is practically justified. It leads to results of acceptable accuracy even when dealing with complicated flow phenomena.
- 2-Nonlinearity of aerodynamic reactions ,including pitch damping, is significant in low aspect ratio configurations.
- 3-Besides its favourable contribution to aerodynamic forces,nonlinearity favourably contributes to pitch damping.
- 4-Fuselages induced nonlinearity effectively contributes to nonlinearity of aerodynamic characteristics of their aircraft assemblies.
- 5-For measured configurations and given test conditions,dimensional pitch damping linearly varies with flow velocity and the nondimensional damping in pitch derivative is independent on nondimensional frequency.

REFERENCES

- 1- Etkin,B.:Dynamics of atmospheric flight.John Wiley,1972.
- 2- Smetana,F.,Summy,D.,Jobson,W.:Riding and handling qualities of light aircraft. NASA CR -1975 . March 1972.
- 3- Abdelhamid,O.A:Measuring of damping derivatives of partial assembly of a jet-plane fuselage tail units. VZLU report 2180/75
- 4- Abdelhamid,O.A.: Possibilities of measurement of aircraft stability derivatives in aerodynamic tunnels.VAAZ,Brno 1973.
- 5- Pope,A.,Harper,J.:Low speed wind tunnel testing.John Wiley,1966.
- 6- Danek,M.:Flow downwash at horizontal tail position of quickly oscillating airplane. VAAZ , Brno 1956.
- 7- Thwaites,B.:Incompressible aerodynamics.Oxford,1960.
- 8- Kuchemann,D.:The aerodynamic design of aircraft.Pergamon Press 1978.

LIST OF SYMBOLS

| | |
|-----------------|--|
| C | airplane wing mean aerodynamic chord |
| C_{LW} | lift curve slope of wing-body combination |
| C_{LHT} | lift curve slope of horizontal tail surface |
| J_y | moment of inertia of balance and model around lateral axis |
| k_a | aerodynamic stiffness |
| k_s | spring stiffness |
| S_{HT}/S_w | ratio of horizontal tail area to wing area |
| $x_{cg}-x_{ac}$ | distance between center of gravity and aerodynamic center |
| γ | dynamic pressure ratio at tail |